JOURNAL OF SOLID STATE CHEMISTRY 115, 247–254 (1995)

Crystal Structure and Magnetic Properties of the Ternary Germanide $U_3Co_4Ge_7$: An Intergrowth of $CaBe_2Ge_2$- and Cu_3Au-Type Slabs

R. Pöttgen,*,† B. Chevalier,*,[1] P. Gravereau,* B. Darriet,* W. Jeitschko,*,† and J. Etourneau*

*Laboratoire de Chimie du Solide du CNRS, Université Bordeaux 1, 351, Cours de la Libération, 33405 Talence Cedex, France; and †Anorganisch-Chemisches Institut, Universität Münster, Wilhelm-Klemm-Straße 8, 48149 Münster, Germany

Received March 21, 1994; in revised form July 26, 1994; accepted August 2, 1994

An electon and X-ray diffraction investigation of powder and single crystals shows that $U_3Co_4Ge_7$ crystallizes in a tetragonal structure with the space group $I4/mmm$,: $a = 410.87(7)$ pm, $c = 2747.7(9)$ pm, $V = 0.4638(2)$ nm^3, $Z = 2$, $R = 0.039$ for the Rietveld refinement, and $R = 0.050$ for the single-crystal study (373 F values and 21 variables). Its structure shows some similarities with that of $Eu_2Pt_7AlP_{4-x}$ and can be interpreted as an intergrowth of $CaBe_2Ge_2$- and Cu_3Au-type blocks. $U_3Co_4Ge_7$ orders ferro- or ferrimagnetically at 21.5(5) K and exhibits another magnetic transition below 20.5(3) K. Its properties are compared to those observed for other ternary germanides such as UCo_2Ge_2 and UCoGe.

I. INTRODUCTION

In a recent paper, we investigated the $UCo_{2-x}Ge_{2+x}$ system for $-0.2 \leq x \leq 0.5$ (1). This study has allowed us to prepare the two ternary germanides UCo_2Ge_2 and "$U_2Co_3Ge_5$." The former compound shows both a narrow range of homogeneity on the cobalt-rich side and two different crystallographic structures. After annealing at 800°C, UCo_2Ge_2 crystallizes in the tetragonal $ThCr_2Si_2$ type ($I4/mmm$ space group), whereas after melting and quenching its crystal structure has a symmetry lower than $I4/mmm$ (1–4).

The ternary germanide "$U_2Co_3Ge_5$," for which the approximate chemical composition has been determined using microprobe analysis (atomic percentages: U, 21.5%; Co, 28.8%; and Ge, 49.6%), can be considered as a magnetically ordered heavy fermion system (1, 5). The X-ray powder pattern of "$U_2Co_3Ge_5$" could be indexed with a tetragonal unit cell ($a' = 411$ pm and $c' = 917$ pm), but its structural properties are as yet undetermined. In the present paper, we report on the structure determination of this compound using both X-ray diffraction performed on single crystals and powder, and electron diffraction. Our study indicates that the correct chemical composition of this compound is $U_3Co_4Ge_7$. The results of the magnetic measurements obtained on $U_3Co_4Ge_7$ are discussed on the basis of the structure determination reported here.

[1] To whom correspondence should be addressed.

II. SAMPLE PREPARATION

Starting materials for the preparation of $U_3Co_4Ge_7$ were platelets of uranium, cobalt granules, and germanium lumps (all with stated purities >99.9%). A very well crystallized sample was obtained by melting of the elements in the atomic ratio 2U : 3Co : 5Ge in an induction levitation furnace under a purified argon atmosphere. To ensure good homogeneity the resulting ingot was turned over and remelted three times. Then, the sample was sealed in an evacuated silica tube and annealed for 2 weeks at 800°C.

III. RESULTS AND DISCUSSION

III.1. Crystal Structure

III.1.1. TEM investigation. For the investigation in a transmission electron microscope (JEOL 2000 FX), parts of the annealed sample were crushed in methanol and the small crystal fragments were placed on a copper grid covered with an amorphous holey carbon film. Selected-area electron diffraction patterns of the [010] and [−110] zone directions, corresponding to the reciprocal lattice planes $(h0l)^*$ and $(hhl)^*$, are shown in Fig. 1. The diffraction patterns reveal the presence of a body-centered tetragonal phase with the cell parameters $a = 410$ pm and $c = 2740$ pm. The value of the c parameter is roughly three times as great as the one determined for "$U_2Co_3Ge_5$" ($c' = 917$ pm) from X-ray powder diffraction.

III.1.2. Single-crystal X-ray diffraction. The annealed sample of the composition "$U_2Co_3Ge_5$" contained some well developed plate-like crystals. Their Buerger precession diagrams confirmed the tetragonal symmetry, and the only systematic extinctions (hkl observed only with $h + k + l = 2n$) were those for a body-centered

0022-4596/95 $6.00

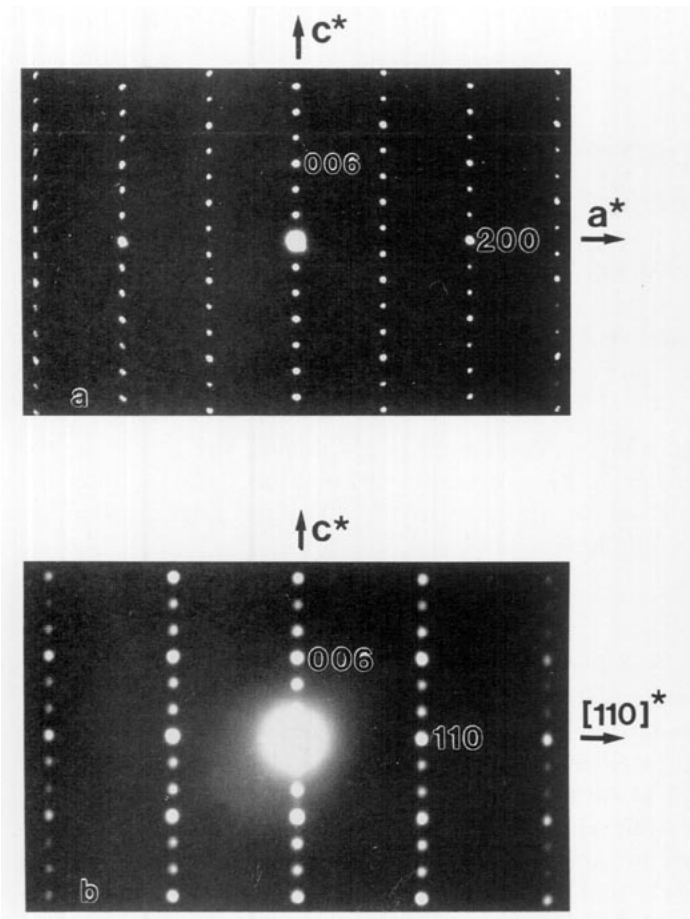

FIG. 1. Typical [010] (a) and [−110] (b) zone axis electron diffraction patterns of $U_3Co_4Ge_7$ microcrystals.

lattice. The structure refinements eventually showed that the space group with the highest symmetry compatible with these extinctions, $I4/mmm - D^{17}_{4h}$, was the correct one.

Intensity data of a crystal with the dimensions 11 × 22 × 88 μm^3 were recorded on an automated four-circle diffractometer (Enraf–Nonius, CAD4) with graphite-monochromated MoK_α radiation, a scintillation counter, and a pulse-height discriminator. Background counts were taken at both ends of each $\theta/2\theta$ scan. A total of 7102 reflections was recorded in the whole reciprocal sphere up to $2\theta = 45°$. An empirical absorption correction was applied from psi-scan data. The ratio of the highest to the lowest transmission was 1.64. After equivalent reflections were averaged ($R_i = 0.072$) and those with $I_0 < 3\sigma(I_0)$ were omitted from the data set, 373 unique reflections remained.

The starting atomic parameters of the uranium atoms were deduced from a Patterson synthesis, while the cobalt and germanium positions were located in subsequent difference Fourier maps. The correct chemical composition of this ternary germanide was found to be $U_3Co_4Ge_7$, with a theoretical density of $d_{calc} = 10.43$ g cm^{-3} and a linear absorption coefficient $\mu(MoK_\alpha) = 783$ cm^{-1}. The structure was refined with a full-matrix least-squares program using atomic scattering factors (6), corrected for anomalous dispersion (7). A parameter correcting the secondary isotropic extinction was refined and applied to the calculated structure factors. The weighting scheme included a factor which accounted for the counting statistics. All atoms were refined with ellipsoidal thermal parameters. In a separate series of least-squares cycles the scale factor was held constant and all occupancy parameters were allowed to vary along with their thermal parameters. The results—occupancy parameters in % (with standard deviations in parentheses) of 100.1(6), 101.7(4), 91(3), 103(2), 104(2), 102(1), and 94(2) for the U1, U2, Co1, Co2, Ge1, Ge2, and Ge3 positions—showed that all occupancies are ideal within four standard deviations, and we assumed again the ideal occupanies for the final cycles. The thermal parameters of all atoms, however, were extremely anisotropic with large B_{11} and B_{22} values and with very small or even negative B_{33} values. This anomaly was judged to be due to the flat shape of the crystals. The structure was then refined with isotropic thermal parameters, followed by a DIFABS absorption correction (8). The final refinement cycles were again with ellipsoidal thermal parameters. The resulting conventional and weighted residuals are $R = 0.050$ and $R_w = 0.056$ for 21 variable parameters and 373 structure factors. A final difference Fourier synthesis showed a value of 3.0 $e/Å^3$ as highest residual density, too close to the U2 position to be suitable for an additional atomic site. It most likely resulted from an incomplete absorption correction of the data. The atomic and thermal parameters are listed in Table 1, and the interatomic distances in Table 2. Listings of the anisotropic thermal parameters

TABLE 1
Atomic Parameters of $U_3Co_4Ge_7$

Atom	Site	x	y	z	z_R[a]	B_{eq}
U1	2a	0	0	0	0	0.04(1)
U2	4e	0	0	0.32999(4)	0.3298(1)	0.18(1)
Co1	4e	0	0	0.1174(2)	0.1173(1)	0.69(5)
Co2	4d	0	1/2	1/4	1/4	0.42(4)
Ge1	2b	0	0	1/2	1/2	0.50(5)
Ge2	8g	0	1/2	0.41959(9)	0.4194(1)	0.69(4)
Ge3	4e	0	0	0.2025(1)	0.2031(2)	0.35(3)

Note. The equivalent isotropic thermal parameters B_{eq} (×100 in units of nm^2) resulting from the single-crystal refinement. Standard deviations in the position of the least significant digit are given in parentheses throughout the paper.

[a] Positional parameters z_R obtained from the Rietveld refinement.

and of the structure factors may be obtained from the authors.

III.1.3. Microprobe examination and Rietveld refinement of the X-ray powder pattern. After the composition of the ternary germanide was established by the single-crystal structure determination a sample with the ideal composition $U_3Co_4Ge_7$ was prepared as described above. Microprobe examinations were carried out in a CAMEBAX scanning electron microscope. The analysis of the sample was based on the measurements of the U $M_{\alpha 1}$, Co $K_{\alpha 1}$, and Ge $K_{\alpha 1}$ X-ray radiations, which were compared with those of UCoGe, used as a reference material. The elemental analyses of the $U_3Co_4Ge_7$ sample gave the following experimental atomic percentages: U, 21.2(6)%; Co, 28.3(8)%; and Ge, 50.5(4)%. These values are in excellent agreement with the ones calculated for the ideal composition (U, 21.43%; Co, 28.57%; Ge, 50.0%).

The germanide was characterized through its Guinier powder pattern. Cu $K_{\alpha 1}$ radiation was used with α-quartz (a = 491.30 pm, c = 540.46 pm) as an internal standard. The lattice constants were refined by least-squares fits of the powder data. To assure proper indexing, the observed pattern was compared with the calculated one (9), assuming the atomic positions as obtained from the single-crystal structure refinement. The lattice constants are a = 410.87(7) pm, c = 2747.7(9) pm, and V = 0.4638(2) nm^3. The values of the lattice constants obtained on the four-circle diffractometer (a = 410.85(3) pm, c = 2748.7(3) pm, and V = 0.4640(2) nm^3) are in good agreement with the powder data.

TABLE 2
Interatomic Distances (pm) in the Structure of $U_3Co_4Ge_7$[a]

U1:	4	Ge1	290.5	Co1:	4	Ge2	229.2
	8	Ge2	301.7		1	Ge3	233.8
	2	Co1	322.6		1	U1	322.6
	4	U1	410.9		4	U2	324.5
	8	U2	550.1				
				Co2:	4	Ge3	243.4
U2:	4	Co2	300.9		4	Co2	290.6
	4	Ge3	303.9		4	U2	300.9
	4	Ge2	320.6				
	4	Co1	324.5	Ge1:	4	U1	290.5
	1	Ge3	350.3		8	Ge2	301.7
	4	U2	410.9				
	4	U2	526.9	Ge2:	2	Co1	229.2
	4	U1	550.1		4	Ge2	290.5
					2	Ge1	301.7
					2	U1	301.7
					2	U2	320.6
				Ge3:	1	Co1	233.8
					4	Co2	243.4
					4	U2	303.9
					1	U2	350.3

[a] Standard deviations are all less than or equal 0.3 pm.

As an additional check for the correctness of the structure we refined the X-ray powder data with the Rietveld technique. The data were collected on a Philips PW 1050 diffractometer using a Bragg–Brentano geometry, a copper target, a diffracted beam graphite monochromator, and a take-off angle of 6°. The diffraction pattern was scanned in steps of 0.02° (2θ) from 18° to 120° with a constant counting time of 40 sec. The Rietveld refinement was performed with the FULLPROF (10) program using the positional parameters of the single-crystal investigation as starting values. Of the variable structural parameters only the lattice constants and the four z parameters were refined, while the thermal parameters were fixed at reasonable values. The refinement confirmed the single-crystal work. The resulting positional parameters are listed in Table 1. The residuals for intensities and structure factors were R_I = 0.039 and R_F = 0.029 for 287 independent reflections and 20 variable parameters. The observed and difference X-ray Rietveld patterns are shown in Fig. 2.

III.1.4. The structure of $U_3Co_4Ge_7$ and its relation to UCo_2Ge_2 and $Eu_2Pt_7AlP_{4-x}$. The crystal structure of $U_3Co_4Ge_7$ is shown in Fig. 3. It can be seen that the uranium atoms form three body-centered subcells stacked on top of each other. The arrangements of the cobalt and germanium atoms also show some similarities. The cell content of the three pseudo-body-centered subcells corresponds to $U_2Co_3Ge_{4.5}$, $U_2Co_2Ge_5$, and again $U_2Co_3Ge_{4.5}$, resulting in the total composition $U_6Co_8Ge_{14} = 2U_3Co_4Ge_7$. The subcell reflections are quite pronounced in the powder pattern (Fig. 2). In the first part of that pattern (up to 2 Θ = 80°) the 15 strongest peaks correspond to subcell reflections, while the superstructure reflections are all very weak.

The structure of $U_3Co_4Ge_7$ is closely related to that of $Eu_2Pt_7AlP_{\sim 3}$ (11), which also can be written $Eu_2Pt_7AlP_{4-x}$ (x = 1.05) to emphasize the correspondence. The unit cells of these structures are shown in Fig. 3. Both structures crystallize in space group $I4/mmm$ and have analogous atomic positions. However, the distribution of the atoms on the corresponding Wyckoff sites is quite different. First, $Eu_2Pt_7AlP_{4-x}$ is a quarternary compound and it also has a larger transition-metal content than the ternary germanide $U_3Co_4Ge_7$. In addition, some significant defects occur for the (4d) position occupied by a P1 atom in the phosphide, while this position is fully occupied in $U_3Co_4Ge_7$. Thus, both structures are not directly comparable and the relationship between these two structures may be called *isopointal* (12, 13).

As can be seen from Fig. 3, the relatively extended unit cell of $U_3Co_4Ge_7$ may be regarded as composed of segments with the composition UGe_3 and UCo_2Ge_2, which

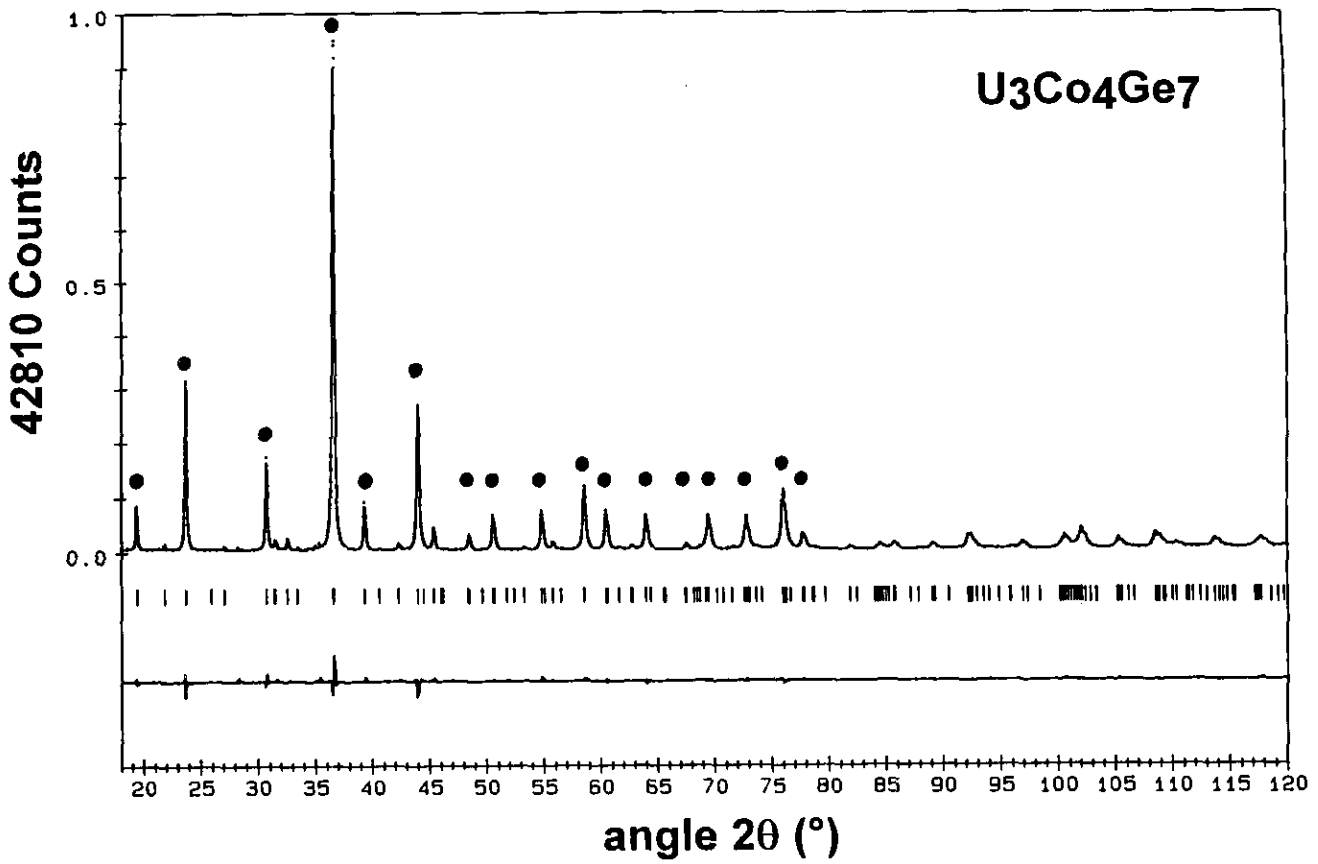

FIG. 2. Observed X-ray powder diffraction pattern and difference spectrum of $U_3Co_4Ge_7$ as obtained after the Rietveld refinement. The location of the reflections is indicated by small vertical lines. The reflections for the subcell with $c' \sim c/3 = 917$ pm are marked with •.

have the same atomic arrangement as the Cu_3Au and $CaBe_2Ge_2$ types. In $Eu_2Pt_7AlP_{4-x}$ the segments have the compositions Pt_3Al and $EuPt_2P_{2-x}$. The segments UGe_3 and Pt_3Al are also known as proper phases, UGe_3 (14) and Pt_3Al (15), crystallizing in the Cu_3Au-type structure, whereas $EuPt_2P_{1.62}$ (16) crystallizes with a stacking variant of the $CaBe_2Ge_2$-type structure (17). The stacking sequence of the Cu_3Au- and $CaBe_2Ge_2$-type slabs in the structures of $U_3Co_4Ge_7$ and $Eu_2Pt_7AlP_{4-x}$ is Cu_3Au–$CaBe_2Ge_2$–Cu_3Au–$CaBe_2Ge_2$*, where the asterisk indicates that the second $CaBe_2Ge_2$ segment is stacked in the inverse direction (when compared to the first one), due to the mirror plane at $z = 1/2$.

A $CaBe_2Ge_2$-type arrangement was also proposed for the high-temperature (HT) form of UCo_2Ge_2 (4) having a c parameter of 929.5 pm. In $U_3Co_4Ge_7$ the c' axis of the $CaBe_2Ge_2$-type segment (as calculated from the positional parameters) is 932 pm and thus similar to that of (HT)-UCo_2Ge_2.

The U1 atoms in $U_3Co_4Ge_7$ have 12 germanium neighbors, 4 at 290.5 pm and 8 at 301.7 pm. The average U1–Ge distance of 298 pm agrees very well with U–Ge bond length of 297.4 pm in UGe_3 (14). In contrast to UGe_3 (a = 420.6 pm), the germanium arrangement around the U1 atoms is not a cube. This UGe_3 unit in $U_3Co_4Ge_7$ is slightly elongated with the tetragonal parameters a'' = 410.9 pm and c'' = 441.9 pm.

The U2 atoms are all within the $CaBe_2Ge_2$-type segment, which corresponds exactly to the cell extended between two Ge2 atoms as shown in Fig. 3. From the Ge2 position a c' parameter of 932 pm can be calculated for this UCo_2Ge_2-segment. This c' parameter is comparable to the translation period c of 929.5 pm of (HT)-UCo_2Ge_2 (4). However, because of the larger cell size and the different symmetry, the $CaBe_2Ge_2$-type segment in $U_3Co_4Ge_7$ is distorted when compared to the ideal $CaBe_2Ge_2$-type structure.

The average U–Co bond lengths of 322.6 and 312.7 pm for U1–Co and U2–Co, respectively, are comparable to the one observed in the (LT) form of UCo_2Ge_2 (Table 3). The U2–Ge distances range from 303.9 to 350.3 pm with an average distance of 316.5 pm. This value is greater than the one determined for the (LT) form of UCo_2Ge_2. Both of these distances are significantly larger than the

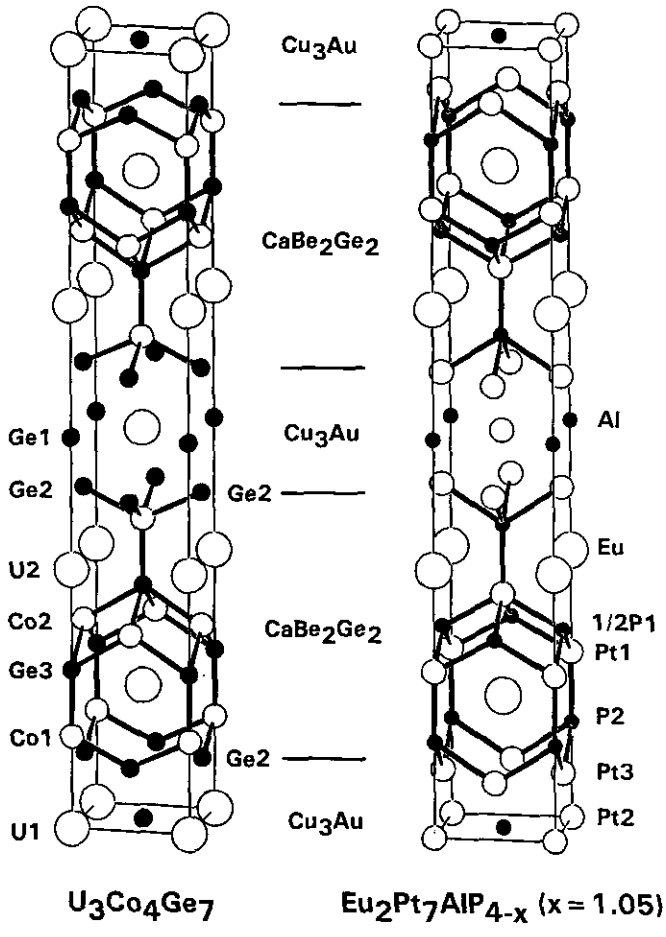

FIG. 3. The crystal structures of $U_3Co_4Ge_7$ and $Eu_2Pt_7AlP_{4-x}$. The stacking sequences of the Cu_3Au- and $CaBe_2Ge_2$-like segments are indicated.

U1–Ge and U–Ge distances existing in the UGe_3 segments of $U_3Co_4Ge_7$ and UGe_3, respectively (Table 3). This result suggests that the overlap between the $5f(U)$ and the s, p, d (Ge) orbitals may be larger for the U1 atoms in $U_3Co_4Ge_7$.

III.2. Magnetic Properties

Magnetization measurements were carried out between 4.2 and 300 K using both a pendulum susceptometer and a SQUID magnetometer. The *ac* susceptibility measurements, in the temperature range from 5 to 30 K, were performed on polycrystalline samples using a Lake Shore Series 7000 AC susceptometer.

III.2.1. dc and ac magnetic measurements. Above 60 K, the temperature dependence of the magnetic susceptibility of $U_3Co_4Ge_7$ can be described by a Curie–Weiss law including a temperature-independent contribution $\chi_0 = 1.14 \cdot 10^{-3}$ emu/(U atom): $\chi = \chi_0 + C/(T - \theta_P)$ with $\theta_P = -16$ K (Fig. 4). The value of the effective paramagnetic moment $\mu_{eff} = (8\ C)^{1/2} = 2.15\ \mu_B$/(U atom), which is low in comparison with those calculated for either divalent (3.26 μ_B) or trivalent (3.58 μ_B) uranium, is comparable with the values reported recently for the other ternary uranium cobalt germanides (HT)-UCo_2Ge_2 (4), $UCo_{2.05}Ge_{1.95}$ obtained after melting and quenching (1), and UCoGe (18, 19) (Table 3). For these compounds, the important value of the χ_0 term (Pauli susceptibility of the conduction electrons, etc.) and the small μ_{eff} moments for the uranium atoms indicate that the $5f(U)$ electrons have an itinerant character.

Figure 5 shows the temperature dependence of the

TABLE 3
Crystallographic, Magnetic, and Thermal Data for Several Compounds of the Uranium–Cobalt–Germanium system

Compound	Crystallographic data[b]				Magnetic data						Ref.
	Str. type	d_{U-U}	d_{U-Co}	d_{U-Ge}	χ_0 (10^{-3} emu/U)	μ_{eff} (μ_B/U atom)	θ_p (K)	Order[a]	T_N or T_C (K)	γ (mJ/K²U)	
UGe_3	Cu_3Au	420.6		297.4	1.15			PP		20.4	(14,23,24)
$U_3Co_4Ge_7$	$U_3Co_4Ge_7$	410.9	U1-Co	U1-Ge	1.14	2.15	−16	F	21(1)	110	This work
			322.6	298.0							
			U2-Co	U2-Ge							
			312.7	316.5							
UCo_2Ge_2 (LT)	$ThCr_2Si_2$	400.8	317.3	309.0		4.31	−340	AF	160		(1)
		402.0	318.2	309.9		4.5	−350	AF	175		(2)
		401.0	318.1	309.3		4.0	−262	AF	174	34	(4)
UCo_2Ge_2 (HT)	$CaBe_2Ge_2$?	404.3			1.8	1.6	−51	P		62	(4)
$UCo_{2.05}Ge_{1.95}$ melted	$CaBe_2Ge_2$?	404.5			1.7	1.83	−29	P			(1)
UCoGe	TiNiSi	354.0	299.7	301.6	1.07	1.73	−10	P		65	(18,20)
	$CeCu_2$				1.2	1.7	−2	P			(19)
UCo	UCo	277.2	282.0		0.73			PP		7.8	(25)

[a] (PP) Pauli paramagnetism, (P) paramagnetism, (AF) antiferomagnetism, and (F) ferro- or ferrimagnetism.
[b] The interatomic distances are given in units of pm.

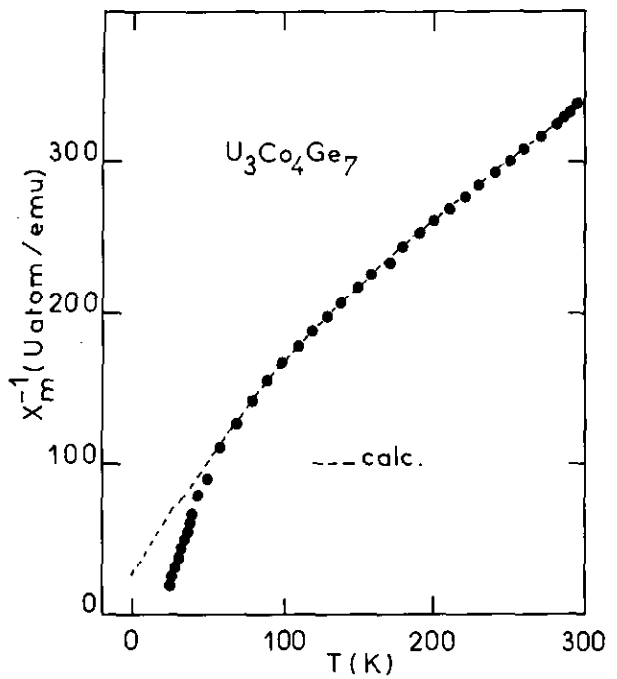

FIG. 4. Temperature dependence of the reciprocal magnetic susceptibility of $U_3Co_4Ge_7$.

magnetization of $U_3Co_4Ge_7$ cooled in an applied magnetic field of $H = 0.01$ T (FC curve). The magnetization increases greatly at $T_C = 21.5(5)$ K characterizing a ferro- or ferrimagnetic transition. For $H = 0.01$ T and at temperatures below 12 K, the magnetization of $U_3Co_4Ge_7$ decreases with temperature, becoming constant. This behavior suggests the presence of some magnetic transitions induced both by temperature and by the applied magnetic field.

Figures 6–8 present the temperature dependences of the in-phase (χ') and out-of-phase (χ'') ac susceptibilities measured at various external fields H. The ac field was equal to 0.5 Oe and the frequency amounted to 125 Hz. For $H = 0$ and 0.03 T, two peaks occur at 20.5(3) and 21.1(3) K in the χ' curve. The positions and amplitudes of these peaks are dependent on the H field: (i) the first peak ($\cong$20.5 K) disappears for $H \geq 0.1$T; (ii) the second peak moves from 21.1 to 24.5 K as the field increases from 0.03 to 0.8 T; (iii) this last peak becomes relatively broad as H increases. From these results, it appears that $U_3Co_4Ge_7$ shows two magnetic ordering transitions with decreasing temperature at least for $H < 0.1$ T. Our first measurements suggest that the magnetic phase diagram of $U_3Co_4Ge_7$ is complex. This behavior could be due to a strong competition between ferromagnetic and antiferromagnetic properties as in UNiGa and UPdSn (21, 22).

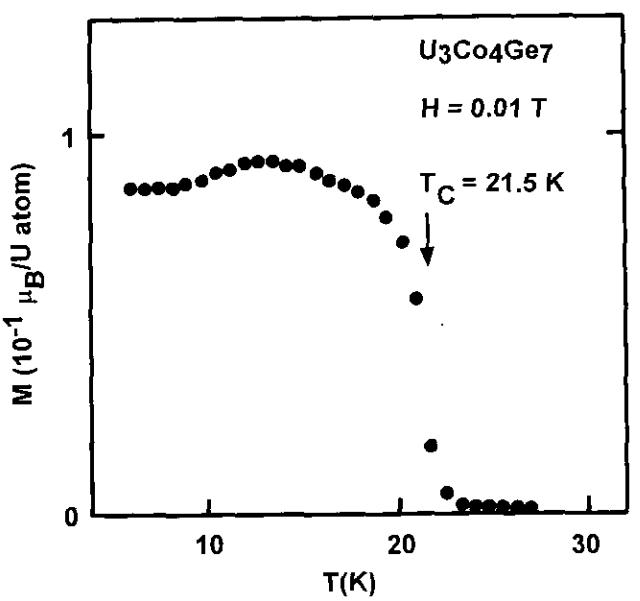

FIG. 5. Temperature dependence of the magnetization of $U_3Co_4Ge_7$ cooled in an applied magnetic field of $H = 0.01$ T.

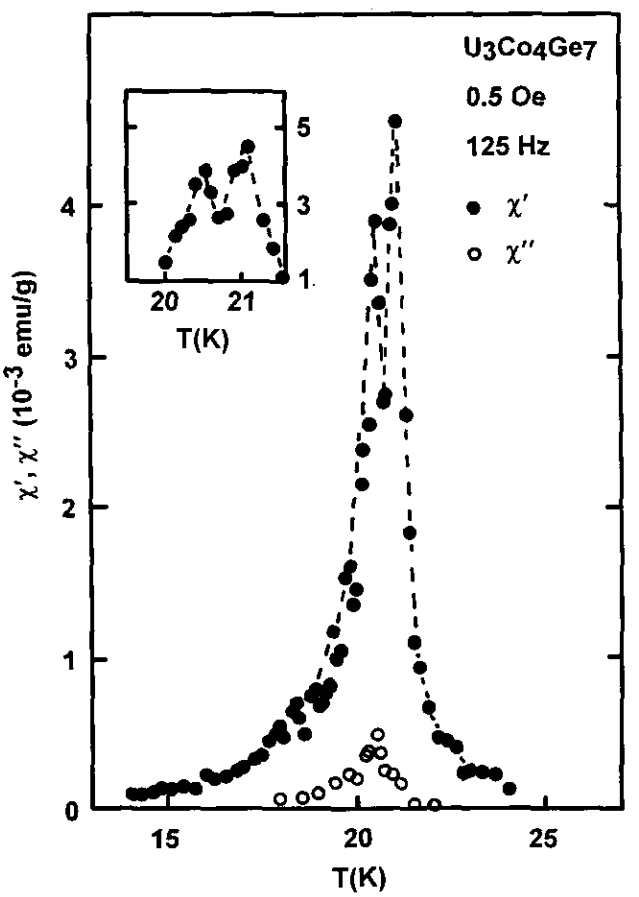

FIG. 6. Temperature dependence of the in-phase (χ') and out-of-phase (χ'') ac susceptibility of $U_3Co_4Ge_7$ (ac field, 0.5 Oe; frequency, 125 Hz).

Other magnetization measurements and neutron diffraction studies are essential to solve this interesting magnetic phase diagram.

III.2.2. Magnetic relation between $U_3Co_4Ge_7$, UCo_2Ge_2, and UCoGe. The magnetic properties of UCo_2Ge_2 are strongly correlated to its structural properties. The (LT) form orders antiferromagnetically with a high Néel temperature whereas the (HT) form exhibits no magnetic ordering down to 1.7 K (Table 3). The relative small value of the effective uranium moment in the (HT) form coupled with an enhanced electronic specific heat coefficient ($\gamma = 62$ mJ/K^2 U atom) prove that the 5*f* states of the uranium atoms are very near to the Fermi level. Similar remarks can be made for $U_3Co_4Ge_7$ and UCoGe. The behavior of this last germanide is close to ferromagnetic; a large magnetic moment of 0.58 μ_B/(U atom) is induced by a field of 35 T (20). Also, $U_3Co_4Ge_7$ can be considered as a magnetically ordered heavy fermion compound (the γ value given in Table 3 is relative to "$U_2Co_3Ge_5$" taken from Ref. (1)). All these results show a great instability of the 5*f* electrons in the ternary uranium cobalt germanides. Small changes of the Fermi level caused for instance by an applied magnetic field or the occurrence of structural transitions produce a drastic effect on their magnetic properties.

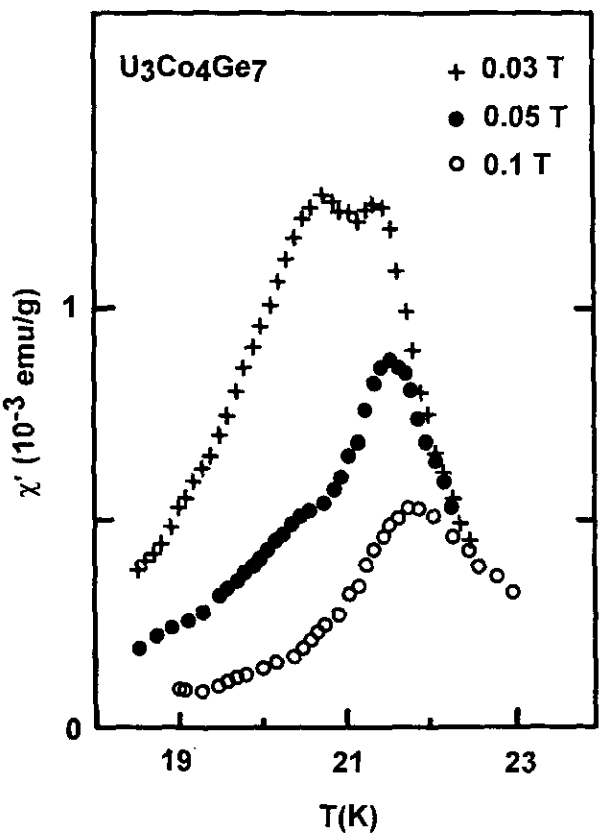

FIG. 7. χ' susceptibility vs temperature for $U_3Co_4Ge_7$ at dc magnetic fields of 0.03, 0.05, and 0.1 T.

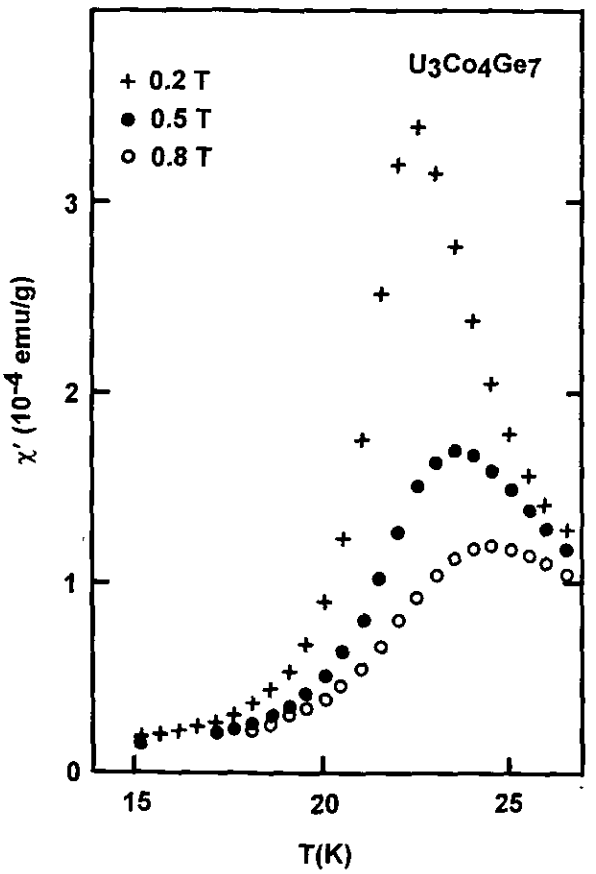

FIG. 8. χ' susceptibility vs temperature for $U_3Co_4Ge_7$ at dc magnetic fields of 0.2, 0.5, and 0.8 T.

In this view it is interesting to discuss the strength of the 5*f*(U)-ligand hybridization, which is directly linked to the U–Co and U–Ge distances observed for these ternary germanides. It is well known that the Pauli paramagnetic behavior of UGe_3 is governed by the existence of short U–Ge distances, leading to a delocalization of the 5*f* electrons (23). In $U_3Co_4Ge_7$ the average U1–Ge distance is similar to that observed in UGe_3 and UCoGe. This suggests that the 5*f*(U1) orbitals are admixed with the electronic states of the germanium atoms explaining the large γ value. In contrast, this hybridization may be smaller for the U2 atoms in $U_3Co_4Ge_7$ because the average U2–Ge distance is greater. The U–Co distances of all ternary germanides mentioned in Table 3 are greater than the corresponding distance in UCo, which displays a Pauli paramagnetic behavior (25). The 5*f*(*U*)–3*d*(Co) hybridization possibly contributes a smaller part on the magnetic properties of these compounds.

IV. CONCLUSION

The crystal structure of $U_3Co_4Ge_7$ can be considered as an intergrowth of $CaBe_2Ge_2$- and Cu_3Au-type slabs. Accordingly, the uranium atoms occupy two unequivalent crystallographic sites, one of which has a similar germanium environment to that observed in UGe_3. The ac magnetic susceptibility measurements reveal two magnetic transitions at 20.5 and 21.1 K and the existence of a complex magnetic phase diagram for $U_3Co_4Ge_7$.

ACKNOWLEDMENTS

We thank Dipl.-Ing. U. Rodewald and Dr. M. H. Möller (*Anorganisch-Chemisches Institut, Universität Münster*) for the data collection on the four-circle diffractometer and L. Trut (Laboratoire de Chimie du Solide du CNRS, Bordeaux) for the collection of the Rietveld data. One of us (R.P.) is grateful to the European Community for a fellowship within the framework of the "Human Capital and Mobility Programme."

REFERENCES

1. E. Hickey, B. Chevalier, B. Lepine, J. Etourneau, M. Antonia Frey Ramos, J. Ferreira da Silva, M. Manuela Amado, and J. B. Sousa, *J. Alloys Comp.* **178,** 413 (1992).
2. M. Kuznietz, H. Pinto, H. Ettedgui, and M. Melamud, *Phys. Rev. B* **40,** 7328 (1989).
3. M. Kuznietz, H. Pinto, and M. Melamud, *J. Magn. Magn. Mater.* **96,** 245 (1991).
4. T. Endstra, G. J. Nieuwenhuys, A. A. Menovsky, and J. A. Mydosh, *J. Appl. Phys.* **69,** 4816 (1991).
5. T. Endstra, Ph. D. Thesis, University of Leiden, The Netherlands, (1992).
6. D. T. Cromer and J. B. Mann, *Acta Crystallogr. Sect. A* **24,** 321 (1968).
7. D. T. Cromer and D. Liberman, *J. Chem. Phys.* **53,** 1891 (1970).
8. N. Walker and D. Stuart, *Acta Crystallogr. Sect. A.* **39,** 158 (1983).
9. K. Yvon, W. Jeitschko, and E. Parthé, *J. Appl. Crystallogr.* **10,** 73 (1977).
10. J. Rodriguez-Carjaval, Collected Abstracts of Powder Diffraction Meeting, Toulouse, France, 1990, p. 127.
11. C. Lux, G. Wenski, and A. Mewis, *Z. Naturforsch. B* **46,** 1035 (1991).
12. L. M. Gelato and E. Parthé, *J. Appl. Crystallogr.* **20,** 139 (1987).
13. E. Parthé and L. M. Gelato, *Acta Crystallogr. Sect. A* **40,** 169 (1984).
14. R. Huch and W. Klemm, *Z. Anorg. Allg. Chem.* **329,** 123 (1964).
15. J. Faber, Jr., G. H. Lander, P. J. Brown, and A. Delapalme, *Acta Crystallogr. Sect. A.* **37,** 558 (1981).
16. G. Wenski and A. Mewis, *Z. Naturforsch. B.* **41,** 38 (1986).
17. B. Eisenmann, N. May, W. Müller, and H. Schäfer, *Z. Naturforsch. B.* **27,** 1155 (1972).
18. B. Lloret, Thesis, University of Bordeaux I, No. 956, (1988).
19. R. Troc and V. H. Tran, *J. Magn. Magn. Mater.* **73,** 289 (1988).
20. K. H. J. Buschow, E. Brück, R. G. van Wierst, F. R. de Boer, L. Havela, V. Sechovsky, P. Nozar, E. Sugiara, M. Ono, M. Date, and A. Yamagishi, *J. Appl. Phys.* **67,** 5215 (1990).
21. V. Sechovsky, L. Havela, L. Jirman, W. Ye, T. Takabatake, H. Fujii, E. Brück, F. R. de Boer, and H. Nakotte, *J. Appl. Phys.* **70,** 5794 (1991).
22. H. Nakotte, E. Brück, F. R. de Boer, P. Svoboda, N. C. Tuan, L. Havela, V. Sechovsky, and R. A. Robinson, *J. Appl. Phys.* **73,** 6551 (1993).
23. D. D. Koelling, B. D. Dunlap, and G. W. Crabtree, *Phys. Rev. B* **31,** 4966 (1985).
24. M. H. van Maaren, H. J. van Daal, K. H. J. Buschow, and C. J. Schinkel, *Solid State Commun.* **14,** 145 (1974).
25. J. W. Chen, R. R. Hake, S. E. Lambert, M. B. Maple, C. Rossel, M. S. Torikachvili, and K. N. Yang, *J. Appl. Phys.* **57,** 3090 (1985).